Proceeding of the 2004 American Control Conference
Boston, Massachusetts June 30 - July 2, 2004

DAC Quantization Noise Reduction for Servo Control Systems in Hard Disk Drives

Wei-Min Lu, *Member, IEEE,* Roger Wood*, Member, IEEE, and* Mantle Yu

Abstract— **In hard disk drive (HDD) servo control systems, quantization noises due to the finite precision of the D/A converter (DAC) driving the VCM contribute a significant portion of the total track mis-registration (TMR). In this paper, a quantization error feedback (QEF) technique to reduce TMR due to DAC quantization noises is introduced). The QEF technique offers a simple method of reshaping the spectrum of this noise to minimize its contribution to TMR. Despite the name, QEF is an effectively feed-forward technique that means that it does not affect or degrade the servo loop response. In addition, the limitation and optimality of different QEF schemes are examined in detail. Simulations reveal that contribution to TMR on an HDD is reduced by more than a factor of ten. Tests have verified the improvement.**

I. Introduction

In hard disk drives (HDD), the digital to analog converter (DAC) driving the voice coil motor (VCM) has limited accuracy. Quantization noises (or roundoff errors) due to the finite precision of the DAC disturb the servo control loop and degrade servo control performance. The DAC quantization noises contribute a significant portion of the total track-misregistration (TMR) in HDD products. Furthermore, for fixed mechanics and servo control bandwidth in a HDD, the power spectrum of TMR due to DAC noises is fixed, and the TMR does not scale with the track density. Therefore, the DAC quantization noise will be a recurring problem as the track density goes higher; techniques to effectively reduce such TMR are desirable.

This paper describes a numerical technique, which goes by the general name of "quantization error feedback" or QEF, to reduce the HDD TMR due to quantization noises arising from a DAC with fixed precision without degrading other desired servo properties. These QEF schemes are implemented entirely within the DSP. In the digital servo control loop, the internal precision of the digital signal processor (DSP) is typically higher (e.g., 16 bits) than that of the DAC (e.g., 12 bits). The lower order bits have to be dropped when the calculated control signal is sent to DAC. In the QEF schemes, the truncated lower order bits, which are referred as the quantization errors, is monitored and accumulated in the DSP. When sufficient error has accumulated, the bits feeding the DAC can be modified in such a way as to largely cancel the effects of the error. In the frequency domain, the effect of the process is to reshape the spectrum of the quantizing noise. The noise seen at the DAC may increase at some frequencies, but its overall contribution to (the mean square value of) TMR is dramatically reduced. Simulations with real HDDs reveal that the contribution to TMR can be reduced by more than a factor of ten with optimal QEF schemes (see Fig. 25). Tests in real HDD products show the TMR improvement.

A kind of QEF technique was also used in the data transmission systems to reduce low frequency content of quantizing errors [2,3]. The purpose and implementation of the QEF technique introduced here for HDDs are different. In this paper, we will examine the QEF schemes from control theoretical point of view in order that we fully understand the options available for reducing TMR due to DAC quantization noise. Despite the name, QEF is an effective feed-forward technique; therefore, it does not affect the servo loop performance. In addition, we will also examine the limitation and optimality of the QEF technique; an algorithm that gives optimal QEF schemes is developed. It should be pointed out that even though the QEF technique is proposed for dealing with quantization noise in HDD servo control system, the methodologies and results can be applied to general digital control systems to deal with noises in the control input.

The structure of this paper is organized as follows: In Section 2, we will examine the basic properties of DAC quantization error, and motivate the use of quantization error reduction techniques. In Section 3, we will introduce the basic concepts of the QEF technique. In Section 4, we will give more detailed analysis about QEF technique with general structures, in particular, we will discuss the limitations of using the QEF technique to reduce the impact of quantization noises, and develop an algorithm to derive the optimal QEF filter resulting in maximal TMR reduction. In Section 5, we will give some test results of the QEF technique on real HDDs.

II. DAC Quantization Noise

2.1. D/A Quantization Error

A simplified block diagram of the HDD servo system is given in Fig.1. In HDD servo system, the DSP has higher precision than the A/C converter (DAC) does. Therefore, only the most significant bit (MSB) part of the calculated control signal is sent to the D/A converter, the least significant bit (LSB) part is truncated (rounded off). The error (LSB) due to the DAC truncation is referred as

Manuscript received September 22, 2003. The authors are with the Advanced Technologies, Hitachi GST, Inc., San Jose, CA 95193 (e-mail: wei-min.lu@hgst.com; roger.wood@hgst.com; mantle.yu@hgst.com).

DAC quantization error, denoted as *QE* in the following discussion.

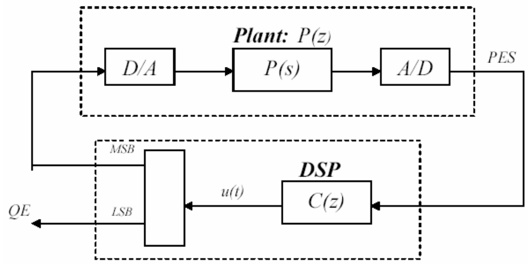

Fig. 1. Digital Servo Systems for HDD

According to Widrow, the quantization noise *QE(t)* can be modeled as a white random process having a uniform probability density in [$-q/2$, $q/2$], where $q=2^l c$ with c being the quantization resolution in DSP, and l being the number of LSB bits [4]. In particular, its mean value is:

$$E(QE(t))=0,$$

and its variance satisfies

$$\delta_{QE}^2 = E\{(QE - E(QE))^2\} = \frac{q^2}{12},$$

The autocorrelation function is given as follows,

$$R_{QE}(\tau) = E\{QE(t)QE(t+\tau)\} = \frac{q^2}{12},$$

if $\tau = 0$; otherwise $R_{QE}(\tau) = 0$. Power density spectrum is given as follows:

$$S_{QE}(\omega) = \sum_{\tau=-\infty}^{\infty} R_{QE}(\tau) e^{-i\tau\omega} = R_{QE}(0) = \frac{q^2}{12}.$$

2.2. Impact of the Quantization Noise on TMR

The block diagram in Fig.1 can be redrawn as the block diagram in Fig.2.

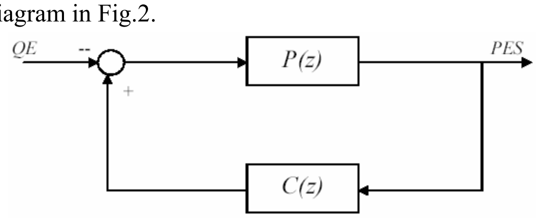

Fig. 2. Equivalent Block Diagram for HDD Servo Systems

Therefore, the TMR due to quantization error of D/A can be represented by

$$PES(z)=H(z)\cdot QE(z),$$

where *H(z)* is the transfer function from *QE* to *PES*:

$$H(z) = \frac{-P(z)}{1-P(z)C(z)},$$

P(z) is the transfer function of the plant, which is dominated by a double-integrator; in this section, we will assume it is a double integrator. The magnitude of TMR or position error signal (*PES*) is measured by its mean square value (or variance), which can be represented by

$$E(PES^2(t)) = \frac{1}{\omega_n}\int_0^{\omega_n} S_{PES}(\omega)d\omega,$$

where ω_n is the Nyquist frequency, which is normalized as π in this paper. Thus the mean square value of TMR is the average power of the signal, which is determined by its power spectrum density function:

$$S_{PES}(\omega) = \| H(e^{i\omega}) \|^2 \, S_{QE}(\omega),$$

As the quantization noise is represented as white noise as discussed in the previous subsection, the shape of power spectrum of TMR depend solely on the frequency response of the system:

$$S_{PES}(\omega) = \| H(e^{i\omega}) \|^2 \frac{q^2}{12}.$$

The typical frequency response of the closed loop system from *QE* to *PES* has a shape of a low pass filter, Fig. 3 shows the typical frequency response from quantization error to TMR for a HDD.

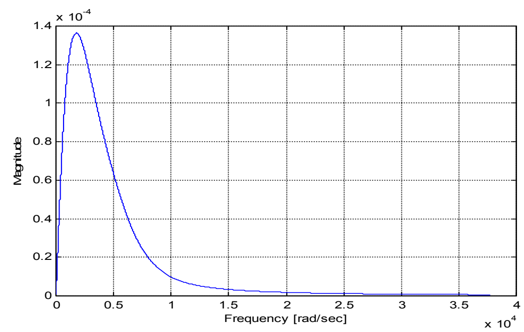

Fig.3. Frequency Response from Quantization Noise to TMR

The power of TMR due to DAC quantization noise is concentrated at lower frequencies. Therefore, the reduction of the average power of *PES* can be achieved by reshaping the power spectrum density function of TMR. Since any alteration of the frequency response of the closed loop transfer function may change other desired properties of the servo systems, desirable techniques for TMR reduction should be those that are able to reshape the power spectrum of the input noise *QE* and reduce the average power of *PES* in the frequency range of interest. In the following, we will focus on such a technique: QEF.

III. Quantization Noise Feedback

3.1. What is QEF?

The idea of QEF is illustrated with the block diagram in Fig. 4. With this technique, the quantization error is monitored and accumulated (integrated) in the DSP. When sufficient error has accumulated, i.e., an MSB is generated, it is added to the original MSB feeding the DAC.

Note that in this QEF scheme, the QE signal is integrated once, we will call this scheme single-integrator QEF. It is also noted that a double integrator scheme also be used for reducing TMR [6].

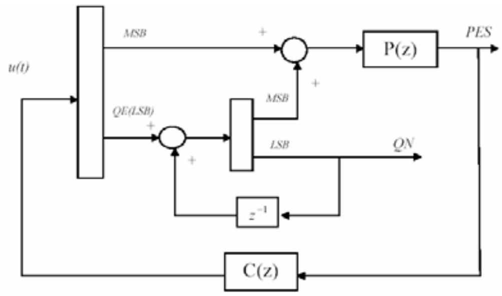

Fig. 4. QEF Technique for TMR Reduction: Single Integrator

Fig. 5 shows the ideal power spectrums of TMR due to quantization error with single-integrator QEF (lower curve) and without any QEF (upper curve), respectively, for an HDD. The TMR reduction is significant.

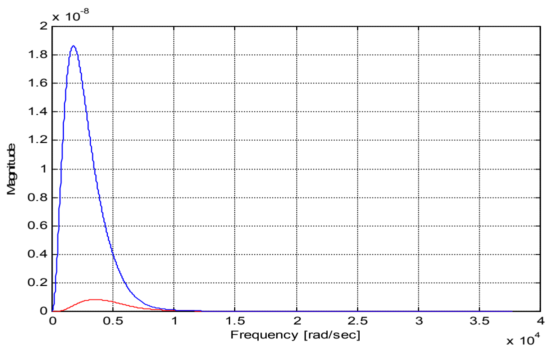

Fig.5. TMR due to Quantization Error with/without QEF

3.2. QEF is a Feedforward Scheme

To help explain the QEF technique, the QEF scheme discussed earlier (Fig.4) is equivalently represented as the block diagram in Fig.6.

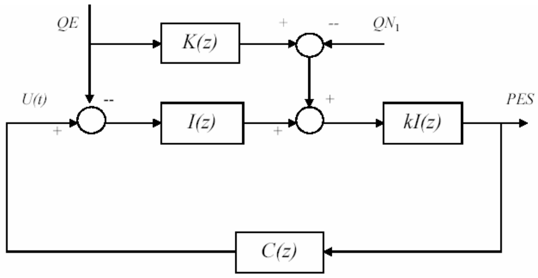

Fig. 6. QEF: Equivalent Block Diagram

In this block diagram, the double-integrator plant is decomposed into two integrators: $P(z)=kI^2(z)$, and $K(z)=I(z)$, where $I(z)$ is a discrete-time integrator: $I(z)=\frac{1}{1-z^{-1}}$. QN_1 can also be interpreted as the truncation error (LSB) of QE after integration in the above block diagrams; as the internal signal driven the block $kI(z)$ should be MSB. Note that QN_1 is exactly the same signal as QN_1 in the diagram in Fig. 3. In the following analysis, QN_1 is white noise with the similar stochastic properties as QE under Widrow's assumption, in particular,

$$S_{QN_1}(\omega)=S_{QE}(\omega)=\frac{q^2}{12}.$$

The control scheme shown in the block diagram is actually feedforward control which does not alter closed loop transfer function. As the prefilter $K(z)$ in this case is a single discrete time integrator.

In the following we refer the QEF technique in Fig.3 as single integrator QEF. In fact, the single integrator QEF is an optimal feedforword control scheme in the sense that the prefilter $K(z)=I(z)$ in Fig. 4 is optimally chosen such that the resulting PES has minimal value [6].

IV. LIMITATION AND OPTIMALITY OF QEF

4.1. A General Structure of QEF

In the previous section, we introduced a single integrator QEF scheme. A general structure for QEF schemes is shown in Fig.14. Note that the feedback loop in the error accumulation operation has at least one pure delay so that the operation is implementable.

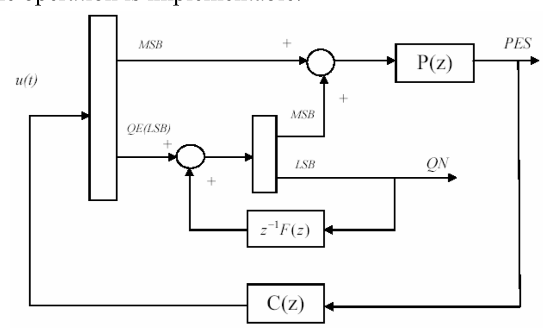

Fig. 14. QEF Technique for TMR Reduction

In this block diagram, QN is truncation error (LSB) of QE after filtering. Note that QN is white noise with similar stochastic properties to QE under Widrow's assumption, in particular,

$$S_{QN}(\omega)=S_{QE}(\omega)=q^2/12.$$

4.2. Optimal QEF Filter and Approximations

Consider the general QEF scheme in Fig. 14. In this structure, the feedback loop gain is $z^{-1}F(z)$, where $F(z)$ is a filter whose transfer function is assumed to be a real rational function which is analytic and bounded in $\{z:\|z\|\geq 1\}$. To explore the limitation of the general QEF schemes, let's look at the possible optimal choice of the filter $F(z)$. With some block diagram manipulation, one can equivalently transform the block diagram in Fig. 14 to the feedforward block diagram in Fig.15.

It is noted that in the above figure, the quantization noise QN is reshaped by the general filter, $1-z^{-1}F(z)$, resulting in disturbance GQE entering the system as

$$GQE(z)=(1-z^{-1}F(z))\cdot QN(z).$$

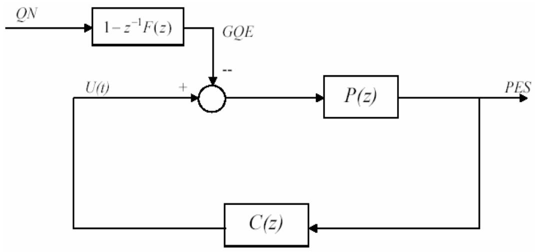

Fig. 15. General QEF: Equivalent Block Diagram

Therefore, the TMR due to quantization error becomes

$$PES(z)=\frac{-P(z)}{1-P(z)C(z)}GQE(z)=H(z)\cdot(1-z^{-1}F(z))\cdot QN(z),$$

where $H(z)$ is the transfer function from QE to PES in the original block diagram. QN is white noise with similar stochastic properties to QE and

$$S_{PES}(\omega)=\|(1-e^{-j\omega}F(e^{j\omega}))H(e^{j\omega})\|^2\ S_{QN}(\omega);$$

the variance of PES is as follows:

$$E(PES^2(t))=\frac{1}{\pi}\int_0^{\pi}S_{PES}(\omega)d\omega=\frac{q^2}{12\pi}\int_0^{\pi}\|(1-e^{-j\omega}F(e^{j\omega}))H(e^{j\omega})\|^2\ d\omega.$$

One can see that

$$\min_F E(PES^2(t))=\min_F\left(\frac{q^2}{12\pi}\int_0^{\pi}\|(1-e^{-j\omega}F(e^{j\omega}))H(e^{j\omega})\|^2\ d\omega\right)=0,$$

where the minimal is achieved (mathematically) with $F(e^{j\omega})=e^{j\omega}$, or $F(z)=z$. Therefore, the (mathematically) optimal filter $F(z)$ is a forward shift operator. Thus, the "optimal" feedback loop gain is identity without any delay. However, it is not implementable, because the QEF feedback loop should contain at least a delay operator. In the following, we will examine how the optimal QEF filter can be approximated by an implementable filter.

Given $a>0$, for all z satisfying $\|1-\frac{z^{-1}}{a}\|<1$, we have the following expansion :

$$z=\frac{1}{z^{-1}}=\frac{1/a}{1-(1-z^{-1}/a)}=\frac{1}{a}\left(1+(1-\frac{z^{-1}}{a})+(1-\frac{z^{-1}}{a})^2+(1-\frac{z^{-1}}{a})^3+\cdots\right).$$

In particular, the n-th order approximation $F(z)$ to z yields:

$$1-z^{-1}F(z)=1-z^{-1}\frac{1}{a}\left(1+(1-\frac{z^{-1}}{a})+(1-\frac{z^{-1}}{a})^2+\cdots+(1-\frac{z^{-1}}{a})^n\right)=(1-\frac{z^{-1}}{a})^n$$

If $a=1$, then the single and double integrator QEF schemes as discussed earlier are recovered with $n=1$, 2, respectively. As $n\to\infty$, the feedback loop gain $1-z^{-1}F(z)$ is convergent to the optimal filter, 0, at the following frequencies:

$$\{\omega:\|1-\frac{e^{-j\omega}}{a}\|<1,\ 0\le\omega\le\pi\}.$$

In particular, if $a=1$, the convergent frequencies are $[0, \pi/3)$. This interprets why the power at the lower frequencies ($\omega\in[0, \pi/3)$) is reduced and enlarged at the higher frequencies ($\omega\in[\pi/3, \pi]$) for both single integrator and double integrator QEF. We also see that the larger a is, the bigger the convergent set; in particular, as $a\to\infty$, the convergent frequency set approaches $[0, \pi/2)$.

4.3. Limitations of QEF Technique

In the following, we will assume the filter $F(z)$ used in the QEF filter has the following expansion:

$$F(z)=f_1+f_2z^{-1}+f_3z^{-2}+\cdots.$$

The reduction of the power of quantization error at some frequencies is at the cost of enlargement of the power at other frequencies. In fact, this is a fundamental limitation for implementable QEFs. This observation is stated in the following statement [6].

<u>QEF Limitation (Spectrum Shaping)</u>

For all implementable QEF schemes, i.e., the filter F(z) in Fig. 12 is a real rational function analytical and bounded in $\{z:\|z\|\ge1\}$, the power spectrum $S_{GQE}(\omega)$ of shaped noise, $GQE(z)=(1-z^{-1}F(z))QN(z)$ with QN being the white quantization noise, always satisfies:

$$\frac{1}{\pi}\cdot\int_0^{\pi}\ln(S_{GQE}(\omega))d\omega=\text{constant},$$

where the constant is independent of the choice of the filter $F(z)$. The proof of the above statement is given in the [6].

In the following, we will examine the limitation of the TMR reduction. The PES with the general structure of the QEF filter is represented as follows:

$$PES(z)=H(z)\cdot(1-z^{-1}F(z))\cdot QN(z)=:\Theta(z)\cdot QN(z),$$

where $H(z)$ is the transfer function from QE to PES in the original block diagram. The power spectrum of PES is

$$S_{PES}(\omega)=\|(1-e^{-j\omega}F(e^{j\omega}))H(e^{j\omega})\|^2\ S_{QN}(\omega),$$

the variance of PES can be obtained by the following formulation:

$$E(PES^2(t))=\frac{q^2}{12\pi}\int_0^{\pi}\|(1-e^{-j\omega}F(e^{j\omega}))H(e^{j\omega})\|^2\ d\omega=\frac{q^2}{12\pi}\int_0^{\pi}\|\Theta(e^{j\omega})\|^2\ d\omega.$$

If the transfer function $\Theta(z)$ from QE to PES is represented as: $\Theta(z)=p_0+p_1z^{-1}+p_2z^{-2}+\cdots$

i.e., its impulse response is $\{p_i\}_{i=1}^{\infty}$, then from Parseval's identity , one has

$$\frac{1}{\pi}\int_0^{\pi}\|\Theta(e^{j\omega})\|^2\ d\omega=\sum_{i=0}^{\infty}p_i^2.$$

Let the closed loop transfer function $H(z)$ satisfies

$$H(z)=z^{-m}\left(h_0+\frac{b_{k-1}z^{k-1}+\cdots+b_1z+b_0}{z^k+a_{k-1}z^{k-1}+\cdots+a_1z+a_0}\right):=z^{-m}H_0(z),$$

for some nonnegative integer m; i.e., there are m pure delays in the closed loop transfer function. Thus,

$$\begin{aligned}H_0(z)&=h_0+\frac{b_{k-1}z^{k-1}+\cdots+b_1z+b_0}{z^k+a_{k-1}z^{k-1}+\cdots+a_1z+a_0}\\&=h_0+\frac{b_{k-1}z^{-1}+\cdots+b_1z^{-(k-1)}+b_0z^{-k}}{1+(a_{k-1}z^{-1}+\cdots+a_1z^{-(k-1)}+a_0z^{-k})}\\&=h_0+h_1z^{-1}+\cdots\end{aligned}$$

for some $\{h_i\}_{i=1}^{\infty}$. One immediately conclude

QEF Limitation (TMR Reduction)

For the QEF schemes considered in this section, the mean square value of PES always satisfies

$$E(PES^2(t)) \geq \frac{q^2}{12} \cdot h_0^2 \cdot$$

The proof of the statement is given in [6]. It gives a TMR lower bound using the QEF techniques.

4.4. Optimal TMR Reduction via QEF

In this section, we will examine with given QEF structure, what is the best QEF filter in the sense the TMR due to quantization noise is reduced. In the following, we will consider the case where the QEF filter $F(z)$ is an FIR filter:

$$F(z) = f_1 + f_2 z^{-1} + \cdots + f_n z^{n-1}.$$

Denote $f = [f_n \quad f_{n-1} \quad \cdots \quad f_1]^T$, then we need to find an optimal vector f, such that

$$f^* = \arg\min_f E(PES^2(t)) = \arg\min_f \left(\frac{q^2}{12\pi}\int_0^{\pi} \|\Theta(e^{j\omega})\|^2\, d\omega\right) \cdot$$

To find out the optimal solutions, we first show how to compute the mean square value of PES in terms of the Parseval's identity from transfer function. We first need to derive the time domain equation for the transfer function:

$$\Theta(z) = H(z)\cdot(1 - z^{-1}F(z)) = (1 - z^{-1}F(z))\cdot H(z),$$

where the transfer function of the closed loop system $H(z)$ has m pure delays as given in the previous subsection:

$$H(z) = z^{-m}\left(h_0 + \frac{b_{k-1}z^{k-1} + \cdots + b_1 z + b_0}{z^k + a_{k-1}z^{k-1} + \cdots + a_1 z + a_0}\right) := z^{-m} H_0(z) \cdot$$

Let $\Theta_0(z) = (1 - z^{-1}F(z))\cdot H_0(z)$, then $\Theta(z) = z^{-m}\Theta_0(z)$. Define

$$A_1 = \begin{bmatrix} 0 & 1 & 0 & \cdots & 0 \\ 0 & 0 & 1 & \cdots & 0 \\ \vdots & & \cdots & & \vdots \\ 0 & 0 & 0 & \cdots & 1 \\ 0 & 0 & 0 & \cdots & 0 \end{bmatrix}_{n\times n}, \quad B_1 = \begin{bmatrix} 1 \\ 0 \\ 0 \\ \vdots \\ 0 \end{bmatrix}_{n\times 1},$$

$$C_1 = -[f_n \quad f_{n-1} \quad \cdots \quad f_1], \qquad D_1 = 1.$$

and

$$A_2 = \begin{bmatrix} 0 & 1 & 0 & \cdots & 0 \\ 0 & 0 & 1 & \cdots & 0 \\ \vdots & & \cdots & & \vdots \\ 0 & 0 & 0 & \cdots & 1 \\ -a_0 & -a_1 & -a_2 & \cdots & -a_{k-1} \end{bmatrix}, \quad B_2 = \begin{bmatrix} 1 \\ 0 \\ 0 \\ \vdots \\ 0 \end{bmatrix}_{k\times 1},$$

$$C_2 = -[b_{k-1} \quad b_{k-2} \quad \cdots \quad b_0], \quad D_2 = h_0.$$

Therefore, the $(n+k)$-th order state space realization of the transfer function $\Theta_0(z) = (1 - z^{-1}F(z))\cdot H_0(z)$ is:

$$\begin{cases} x(t+1) = Ax(t) + Bu(t) \\ y(t) = Cx(t) + Du(t) \end{cases}$$

where state $x = \begin{bmatrix} x_1 \\ x_2 \end{bmatrix}$, and coefficient matrix:

$$A = \begin{bmatrix} A_1 & B_1C_2 \\ 0 & A_2 \end{bmatrix}, \quad B = \begin{bmatrix} B_1D_2 \\ B_2 \end{bmatrix}, \quad C = [C_1 \quad D_1C_2], \quad D = D_1D_2.$$

Now with the state space equation, one can calculate the impulse response of the system; i.e., for the input $\{u(t)\}$ with $u(0)=1$, and $u(t)=0$ for $t>0$, the output response $\{y(t)\}$ can be calculated interms of A, B, and C. Therefore,

$$\begin{aligned} \frac{1}{\pi}\int_0^{\pi} \|\Theta(e^{j\omega})\|^2\, d\omega &= \frac{1}{\pi}\int_0^{\pi} \|e^{-jm\omega}\Theta_0(e^{j\omega})\|^2\, d\omega \\ &= \frac{1}{\pi}\int_0^{\pi} \|\Theta_0(e^{j\omega})\|^2\, d\omega = \sum_{i=0}^{\infty} p_i^2 = \sum_{i=0}^{\infty} y^2(i) \\ &= D^2 + \sum_{i=1}^{\infty} CA^{i-1}BB^T(A^T)^{i-1}C^T \\ &= D^2 + C\left(\sum_{i=1}^{\infty} A^{i-1}BB^T(A^T)^{i-1}\right)C^T \\ &=: D^2 + CLC^T, \end{aligned}$$

where $L = \sum_{i=1}^{\infty} A^{i-1}BB^T(A^T)^{i-1}$ satisfies Lyapunov equation:

$$ALA^T - L + BB^T = 0.$$

Notice that in the state space equation, the matrices A, B, and D are known, so L can be solved in the Lyapunov equation; part of the matrix C depends on the unknown, f, in fact,

$$C = [C_1 \quad D_1C_2] = [-f \quad C_2].$$

Suppose the matrix $L > 0$ is partitioned as

$$L = \begin{bmatrix} L_{11} & L_{12} \\ L_{21} & L_{22} \end{bmatrix};$$

also notice that $D = D_1D_2 = h_0$, one has

$$\begin{aligned} E(PES^2(t)) &= \frac{q^2}{12\pi}\int_0^{\pi} \|\Theta(e^{j\omega})\|^2\, d\omega = \frac{q^2}{12}(D^2 + CLC^T) \\ &= \frac{q^2}{12}(fL_{11}f^T - 2C_2L_{12}f^T + C_2L_{22}C_2^T + h_0^2). \end{aligned}$$

Then the optimal solution f^* satisfies:

$$\frac{\partial E(PES^2(t))}{\partial f} = \frac{q^2}{12}(2f^*L_{11} - 2C_2L_{12}) = 0,$$

or $f^* = C_2L_{12}L_{11}^{-1}$, and

$$\min_f E(PES^2(t)) = \frac{q^2}{12}(C_2(L_{22} - L_{12}L_{11}^{-1}L_{21})C_2^T + h_0^2).$$

L is positive definite, then $L_{22} - L_{12}L_{11}^{-1}L_{21} > 0$, so

$$\min_f E(PES^2(t)) = \frac{q^2}{12}(C_2(L_{22} - L_{12}L_{11}^{-1}L_{21})C_2^T + h_0^2) \geq \frac{q^2}{12}\cdot h_0^2,$$

which again confirms the QEF TMR Limitation statement.

Optimal QEF Algorithm:

1. Construct state space matrices B_2, D_2, A, and B.
2. Solve the following Lyapunov equation:

$$ALA^T - L + BB^T = 0$$

to get the solution $L = \begin{bmatrix} L_{11} & L_{12} \\ L_{21} & L_{22} \end{bmatrix}$.

3. Find the optimal filter coefficients:

$$f^* = C_2 L_{12} L_{11}^{-1}.$$

4. The optimal solution is given by:

$$\min_f E(PES^2(t)) = \frac{q^2}{12}(C_2(L_{22} - L_{12}L_{11}^{-1}L_{21})C_2^T + h_0^2).$$

The above algorithm is used to calculate the optimal QEF schemes for Sailfin HDD products. The reduction of TMR v.s. the order of optimal filter is illustrated in figure 25.

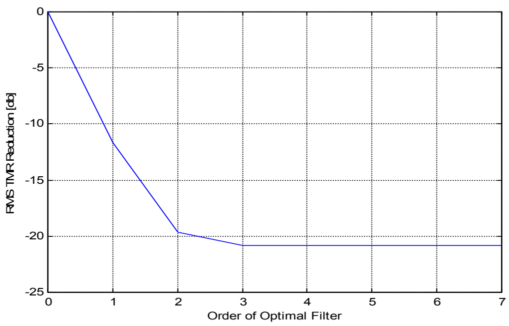

Fig. 25. TMR Reduction v.s. Order of QEF Filter

V. TEST WITH REAL HDDS

In this section, we will present some test results of QEF techniques on Mako HDD. Several first order QEF schemes are implemented. All of the data are taken at OD of the Mako file. The PES (TMR) signals are total NRROs, including TMR due to quantization noise. QEF schemes only reduce TMR due to quantization noises. Therefore, the reduction of the total NRROs is solely due to the reduction of the TMR due to quantization errors. Fig. 27 shows the power spectra of NRROs with QEF (a=1) and without any QEF, respectively.

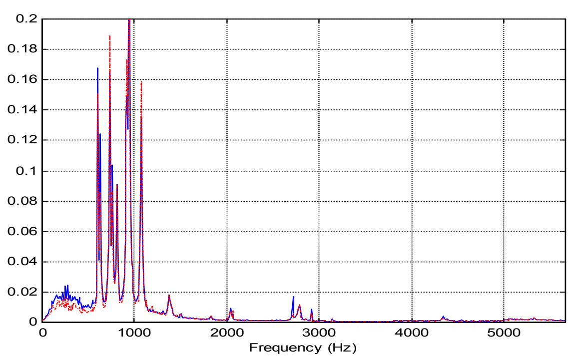

Fig. 27. Power Spectra of NRROs:
Red Curve: a=1, Blue Curve: No QEF

For a changing from 4 to 1, the reduction on root of mean square value (RMS) of the NRRO can be shown in the following diagram in Fig. 29. One can see that the total NRRO RMS is reduced about 3.28% using the single integrator QEF scheme ($a=1$). In fact, the optimal parameter a in the first order QEF is $a^* = 1.0358$.

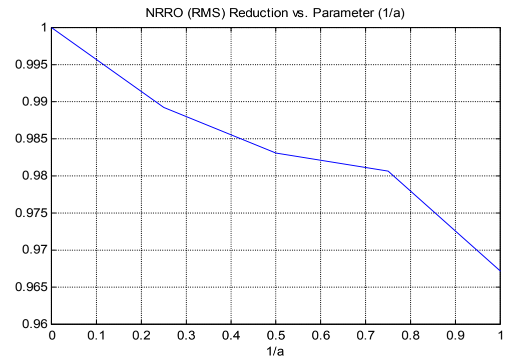

Fig. 29. The NRRO (RMS) Reduction vs. *1/a*

VI. CONCLUSIONS

In this report, we have introduced a QEF technique to reduce the TMR of HDD due to DAC quantization noise without altering or degrading the other desired servo performances. We have examined the limitations of QEF techniques, and give a lower bound for the mean square value of TMR using QEF schemes. We have also derived the optimal QEF filter which minimizes the mean square value of TMR, and an algorithm is provided. From simulation on Sailfin HDD simulation model, the TMR has a RMS reduction by a factor of more than 10 with the optimal QEF schemes. Tests on Mako HDD have verified the improvement (more than 3% reduction on the total NRRO with first order QEF scheme).

REFERENCES

[1] Abramovitch, D., T. Hurst, and D. Henze, “Decomposition of Baseline Noise Sources in Hard Disk Position Error Signals Using PES Pareto Method,” *Proc. of 1997 American Control Conference*, Albuquerque, MN, June 1997.

[2] Cutler, C. C., “Transmission Systems Employing Quantization,” *U.S. Patent,* No.2927962, March 1960.

[3] Eddy, K., J. Steele, and W. Messner, “Bias in Disk Drive Rotary Actuators,” May 1997.

[4] Franklin, G.F., J. D. Powell, and M.L. Workman, *Digital Control of Dynamic Systems*, Addison-Wesley, 1990.

[5] Lang, S. *Complex Analysis*, Springer-Verlag, 1985.

[6] Lu, W.-M., R. Wood, and M. Yu, “Method and apparatus for reducing track misregistration due to digital-to-analog converter quantization noise,” US Patent #6456450, September, 2002.

[7] Spang, III, H.A., P.M. Schultheiss, “Reduction of Quantizing Noise by Use of Feedback,” *IRE Trans. Comm. Syst.,* pp. 373—380, December, 1963.

[8] Yu, M., G. Herbst, and S.-M. Shih, “NODAC Servo System Architecture,” *IBM Internal Report*, San Jose, 1994

[9] Zhou, K., J.C. Doyle, and K. Glover, *Robust and Optimal Control*, Upper Saddle River, NJ: Prentice Hall, 1996.